

# Self-Assembled Ultralarge Millimeter-Sized Graphitic Carbon Rods Grown on Mesoporous Silica Substrate

Zhuxian Yang,<sup>†</sup> Yongde Xia,<sup>†</sup> Yanqui Zhu,<sup>‡</sup> and Robert Mokaya<sup>\*†</sup>

School of Chemistry and School of Mechanical Materials and Manufacturing Engineering, University of Nottingham, Nottingham NG7 2RD, U.K.

Received July 27, 2007. Revised Manuscript Received September 27, 2007

We report the fabrication of new forms of carbon macrostructures: ultralarge (millimeter-sized) self-assembled carbon rods. The rods are obtained during pyrolysis, under chemical vapor deposition (CVD) conditions at 1300 °C, of a carbon precursor (acetonitrile) in the presence of mesoporous silica particles. The rods grow to a length of up to 5 mm and have a diameter of 100–400 μm. The carbon rods grow via the self-assembly of carbon spheres (of diameter 1–2 μm) that are generated from the acetonitrile under the prevailing CVD conditions. A small amount of silica, which functions as substrate (seed or “glue”), is essential for the formation of the large rods. The carbon spheres self-assemble in a closely packed manner to form compact carbon rods that are self-supporting and mechanically robust after removal of the silica particles. The use of a relatively high CVD temperature imparts graphitic characteristics in the carbon rods. The large rods exhibit both high thermal stability and electrical conductivity.

## 1. Introduction

Carbon materials can be prepared with a wide range of structure, property, and morphology characteristics. This versatility means that carbons find use in a variety of applications including in water and air purification, gas storage, catalysis, and as templates or electrode materials. Carbons may be prepared via carbonization of precursors of natural or synthetic origin.<sup>1</sup> Several methods have been explored for the preparation of carbons with tailored porosity (in both the micropore and the mesopore regime) and morphology.<sup>2</sup> Recently, the template carbonization route has attracted much attention for the preparation of porous carbons because it allows the preparation of materials with controlled pore architecture and morphology. The template carbonization synthesis of carbons usually involves the following steps: (a) the preparation of a porous template; (b) the introduction of a suitable carbon source (precursor) into the template pores (internal space) by impregnation (of an organic solution or melt), chemical vapor deposition (CVD), or another synthesis method; (c) the carbonization of the organic–inorganic composite; and (d) the removal of the template. A variety of inorganic porous templates including zeolites,<sup>3</sup> mesoporous silicas,<sup>4</sup> and various molecular carbon sources including

sucrose,<sup>4a</sup> furfuryl alcohol,<sup>3,5</sup> acrylonitrile,<sup>3,5</sup> propylene,<sup>3</sup> pyrene,<sup>5</sup> vinyl acetate,<sup>5</sup> and acetonitrile<sup>6</sup> have been used to prepare porous carbons.

Most carbon materials exist in powder form and therefore require postsynthesis modification or formulation into suitable shapes and forms prior to use in certain applications.<sup>7</sup> Powdered carbon samples therefore have limitations with respect to their ready use in applications such as in catalysis, in high performance liquid chromatography, or as electrode materials. One way of circumventing this limitation is to directly prepare carbon forms (e.g., thin films, monoliths, or rods/needles/wires) that can be readily used without the need for postsynthesis formulation. In particular, the preparation of carbon rods of suitable size that possess appropriate properties (i.e., electrical, thermal, and mechanical) may simplify integration of carbon nanostructures into functional (e.g., electronic) devices. A further challenge in the preparation of carbon rods is the ability to obtain rods that are large

- (4) (a) Ryoo, R.; Joo, S. H.; Jun, S. *J. Phys. Chem. B* **1999**, *103*, 7743. (b) Lee, J.; Yoon, S.; Hyeon, T.; Oh, S. M.; Kim, K. B. *Chem. Commun.* **1999**, 2177. (c) Fuertes, A. B. *J. Mater. Chem.* **2003**, *13*, 3085. (d) Jun, S.; Joo, S. H.; Ryoo, R.; Kruk, M.; Jaroniec, M.; Liu, Z.; Ohsuna, T.; Terasaki, O. *J. Am. Chem. Soc.* **2000**, *122*, 10712. (e) Ryoo, R.; Joo, S. H.; Kruk, M.; Jaroniec, M. *Adv. Mater.* **2001**, *13*, 677. (f) Lee, J.; Han, S.; Hyeon, T. *J. Mater. Chem.* **2004**, *14*, 478. (g) Yang, H. F.; Zhao, D. Y. *J. Mater. Chem.* **2005**, *15*, 1217. (h) Lee, J.; Kim, J.; Hyeon, T. *Adv. Mater.* **2006**, *18*, 2073.
- (5) (a) Alvaro, M.; Atienzar, P.; Bourdelande, J. L.; Garcia, H. *Chem. Commun.* **2002**, 3004. (b) Meyers, C. J.; Shah, S. D.; Patel, S. C.; Sneeringer, R. M.; Bessel, C. A.; Dollahon, N. R.; Leising, R. A.; Takeuchi, E. S. *J. Phys. Chem. B* **2001**, *105*, 2143. (c) Su, F.; Zhao, X. S.; Lu, L.; Zhou, Z. *Carbon* **2004**, *42*, 2821.
- (6) (a) Hou, P.-X.; Orikasa, H.; Yamazaki, T.; Matsuoka, K.; Tomita, A.; Setoyama, N.; Fukushima, Y.; Kyotani, T. *Chem. Mater.* **2005**, *17*, 5187. (b) Xia, Y.; Mokaya, R. *Adv. Mater.* **2004**, *16*, 886. (c) Xia, Y.; Mokaya, R. *Adv. Mater.* **2004**, *16*, 1553.
- (7) (a) Wang, X.; Bozhilov, K. N.; Feng, P. *Chem. Mater.* **2006**, *18*, 6373. (b) Lu, A. H.; Li, W. C.; Schmidt, W.; Schuth, F. *Microporous Mesoporous Mater.* **2006**, *95*, 187. (c) Wang, L.; Lin, S.; Lin, K.; Yin, C.; Liang, D.; Di, Y.; Fan, P.; Jiang, D.; Xiao, F. S. *Microporous Mesoporous Mater.* **2005**, *85*, 136.

\* Corresponding author. E-mail: r.mokaya@nottingham.ac.uk.

<sup>†</sup> School of Chemistry.

<sup>‡</sup> School of Mechanical Materials and Manufacturing Engineering.

- (1) Bansal, C. R.; Donnet, J. B.; Stoeckli, F. *Active carbon*; Marcel Dekker: New York, 1988.
- (2) Kyotani, T. *Carbon* **2000**, *38*, 269.
- (3) (a) Kyotani, T.; Nagai, T.; Inoue, S.; Tomita, A. *Chem. Mater.* **1997**, *9*, 609. (b) Kyotani, T.; Ma, Z. X.; Tomita, A. *Carbon* **2003**, *41*, 1451. (c) Rodriguez-Mirasol, J.; Cordero, T.; Radovic, L. R.; Rodriguez, J. J. *Chem. Mater.* **1998**, *10*, 550. (d) Ma, Z. X.; Kyotani, T.; Tomita, A. *Chem. Commun.* **2000**, 365.

enough. Whereas carbon thin films and monoliths can be prepared at large (millimeter) length scales, this is much more difficult with rods. Nanosized carbon rods have been successfully synthesized,<sup>8</sup> but larger sized rods (up to millimeter scale) present considerable synthesis challenges. It is therefore desirable to explore synthesis routes that are capable of directly generating large (up to millimeter) sized carbon rods. It is also desirable that such rods exhibit good thermal stability and electrical conductivity.

In general, graphitic or partially graphitic (turbostratic) carbons exhibit higher thermal stability and electrical conductivity compared to nongraphitic (amorphous) materials. Carbons with graphitic properties may be obtained via carbonization of suitable precursors at high temperature. Catalytic and noncatalytic pyrolysis of hydrocarbons has been used to prepare carbon spheres.<sup>9</sup> Recently, Kroto and co-workers used the pyrolysis of hydrocarbons containing two to eight carbons, via CVD at 900–1200 °C, for the large scale production of partially graphitic carbon nanospheres and microspheres.<sup>10</sup> In general, carbon spheres generated by carbonization of hydrocarbons via CVD are loosely aggregated.<sup>9,10</sup> Controlled aggregation of the nano- and microsized spheres could be used to generate larger self-supporting and compact carbon macrostructures. We have recently shown that CVD (performed at 550–1100 °C) may be used to prepare carbons exhibiting a wide range of morphology (including hollow shells, solid-core spheres, hollow spheres, nanorods, nanotubules, and nanotubes) by using microporous and mesoporous silicate materials as hard template nanocasts.<sup>6b,c,b,11</sup> We have now explored the nanocasting process at a higher CVD temperature of 1300 °C. Here we report on the use of the CVD nanocasting process for the direct fabrication of new forms of carbon macrostructures: ultralarge millimeter-sized carbon rods. The use of a relatively high CVD temperature ensures that the carbon rods have graphitic characteristics. We assess the role of the silica in the fabrication process and present data on the electrical conductivity of the carbon rods.

## 2. Experimental Section

**2.1. Material Synthesis.** Mesoporous silica SBA-15 with a rod<sup>12</sup> or sphere<sup>13</sup> morphology was prepared as previously reported. Carbon materials were typically prepared as follows: an alumina boat with a known amount of mesoporous silica SBA-15 was placed in a flow-through tube furnace. Two CVD procedures were used. In the first procedure, the furnace was heated to 900 °C at a heating ramp rate of 10 °C/min under flowing argon saturated with acetonitrile and maintained at 900 °C for 3 h. The temperature was then raised to 1300 °C under a flow of argon only and maintained at 1300 °C for 20 h, followed by cooling under argon. The resulting silica/carbon composite was recovered and washed with 10% hydrofluoric (HF) acid several times to remove silica. Finally, the resulting carbon material was dried in an oven at 120 °C. In the second procedure, the furnace was heated to 1300 °C under a flow of argon saturated with acetonitrile and maintained at 1300 °C for 10 h, followed by cooling under argon. Two distinct materials were obtained: powder material that was inside the sample holder and rod-like particles. The resulting silica/carbon composites were washed with 10% HF acid several times to remove the silica template and dried in an oven at 120 °C.

**2.2. Materials Characterization.** Powder X-ray diffraction (XRD) analysis was performed using a Philips 1830 powder diffractometer with Cu K $\alpha$  radiation (40 kV, 40 mA). Nitrogen sorption isotherms and textural properties were determined at –196 °C using nitrogen in a conventional volumetric technique by an ASAP 2020 micromeritics sorptometer. Before analysis the samples were oven-dried at 150 °C and evacuated for 12 h at 200 °C under vacuum. The surface area was calculated using the Brunauer–Emmet–Teller method based on adsorption data in the partial pressure ( $P/P_0$ ) range 0.05–0.2, and total pore volume was determined from the amount of the nitrogen adsorbed at  $P/P_0 \approx 0.99$ . Scanning electron microscopy (SEM) images were recorded using a JEOL JSM-820 scanning electron microscope. Thermogravimetric analysis (TGA) was performed using a Perkin-Elmer Pyris 6 TG analyzer at a heating rate of 2 °C/min under static air conditions. Electrical conductivity measurements were determined at room temperature. Carbon material was pasted with silver between two isolated gold coated glass substrates. The potential and current were supplied and monitored by a CH Instruments electrochemical workstation.

## 3. Results and Discussion

We first ascertained the thermal stability of mesoporous silica and the effect of exposing carbon/silica composites formed at 900 °C<sup>8b</sup> to thermal treatment at 1300 °C. This was done by heating, in a flow-through tube furnace, an alumina boat containing mesoporous silica SBA-15 rods at 900 °C for 3 h under argon saturated with acetonitrile, followed by further heat treatment at 1300 °C under argon only for 20 h. This procedure resulted in the formation of powdered material (designated as sample CR900P). Figure 1 shows representative SEM images of the CR900P carbon sample, after washing with HF to remove silica. The SEM images show the presence of rod-like particles with rough surfaces. The formation of rod-like carbon particles confirmed that, despite the higher temperature and extended CVD duration, the morphology of the mesoporous silica SBA-15 could be generally replicated in the powder carbon

- (8) (a) Yu, C.; Fan, J.; Tian, B.; Zhao, D. Y.; Stucky, G. D. *Adv. Mater.* **2002**, *14*, 1742. (b) Xia, Y.; Yang, Z.; Mokaya, R. *Chem. Mater.* **2006**, *18*, 140.
- (9) (a) Pol, V. G.; Pol, S. V.; Moreno, J. M. C.; Gedanken, A. *Carbon* **2006**, *44*, 3285. (b) Pol, V. G.; Motiei, M.; Gedanken, A.; Calderon-Moreno, J.; Yoshimura, M. *Carbon* **2004**, *42*, 111. (c) Serp, P.; Feurer, R.; Kalck, P.; Kihn, Y.; Faria, J. L.; Figueiredo, J. L. *Carbon* **2001**, *39*, 615. (d) Miao, J. Y.; Hwang, D. W.; Narasimhulu, K. V.; Lin, P. I.; Chen, Y. T.; Lin, S. H.; Hwang, L. P. *Carbon* **2004**, *42*, 813. (e) Qian, H. S.; Han, F. M.; Zhang, B.; Guo, Y. C.; Yue, J.; Peng, B. X. *Carbon* **2004**, *42*, 761. (f) Govindaraj, A.; Sen, R.; Nagaraju, B. V.; Rao, C. N. R. *Philos. Mag. Lett.* **1997**, *76*, 363.
- (10) Jin, Y. Z.; Gao, C.; Hsu, W. K.; Zhu, Y.; Huczko, A.; Bystrzejewski, M.; Roe, M.; Lee, C. Y.; Acquah, S.; Kroto, H.; Walton, D. R. M. *Carbon* **2005**, *43*, 1944.
- (11) (a) Xia, Y.; Yang, Z.; Mokaya, R. *J. Phys. Chem. B* **2004**, *108*, 19293. (b) Yang, Z.; Xia, Y.; Mokaya, R. *Chem. Mater.* **2005**, *17*, 4502. (c) Yang, Z.; Xia, Y.; Mokaya, R. *J. Mater. Chem.* **2006**, *16*, 3417. (d) Yang, Z.; Xia, Y.; Sun, X. Z.; Mokaya, R. *J. Phys. Chem. B* **2006**, *110*, 18424. (e) Yang, Z.; Xia, Y.; Mokaya, R. *J. Am. Chem. Soc.* **2007**, *129*, 1673. (f) Yang, Z.; Xia, Y.; Mokaya, R. *Microporous Mesoporous Mater.* **2005**, *86*, 69.

- (12) Sayari, A.; Han, B. H.; Yang, Y. *J. Am. Chem. Soc.* **2004**, *126*, 14348.
- (13) Zhao, D. Y.; Sun, J.; Li, Q.; Stucky, G. D. *Chem. Mater.* **2000**, *12*, 275.

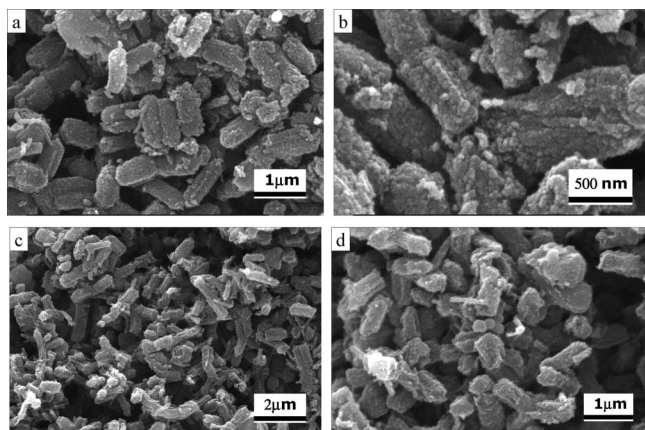


**Figure 1.** SEM images of powder carbon materials prepared via CVD using mesoporous silica SBA-15 rods as template and acetonitrile as carbon source: (a, b) sample CR900P, acetonitrile-saturated argon at 900 °C for 3 h followed by argon only at 1300 °C for 20 h, and (c, d) sample CR1300P, acetonitrile-saturated argon at 1300 °C for 10 h.

materials.<sup>8</sup> The replication of rod-like morphology in sample CR900P also indicated that the silica component of the carbon/silica composite (generated by CVD at 900 °C) is relatively stable to a temperature of 1300 °C.

The preparation of carbon materials via CVD at 1300 °C was performed by heating, in a flow-through tube furnace, an alumina boat containing mesoporous silica SBA-15 rods at 1300 °C for 10 h under a flow of argon saturated with acetonitrile. A visual inspection of the alumina boat (sample holder) after the chemical deposition step at 1300 °C indicated that two distinct materials were obtained: powder material (designated as CR1300P) that was located inside the sample holder and needle or large rod-like particles (designated as CR1300R) that were located either on top of the powder sample or that grew on the rim (edge) or other exposed parts of the alumina boat. Figure 1 shows representative SEM images of the powder CR1300P carbon sample, after washing with HF to remove silica. The SEM images show the presence of rod-like particles with rough surfaces that are similar to those of sample CR900P.

The XRD patterns of the two powder samples (CR900P and CR1300P) are shown in Figure 2. The XRD patterns show that the carbon/silica composites (i.e., before HF treatment, Figure 2A) exhibit a broad peak at  $2\theta$  between 10° and 30°, along with some low intensity peaks at higher  $2\theta$  values. The XRD patterns indicate that the composites consist of amorphous silica (broad halo peak centered at  $2\theta \approx 25^\circ$ ) and turbostratic/graphitic carbon domains (low intensity peaks at  $2\theta > 40^\circ$ ).<sup>8b,11,14</sup> The XRD patterns in Figure 2B indicate that treatment with HF removed the silica, and the resulting powder carbon materials exhibit XRD patterns typical for turbostratic carbon (sample CR900P) and graphitic carbon (sample CR1300P).<sup>8b,11,14</sup> The presence of turbostratic/graphitic carbon is indicated by peaks at  $2\theta = 26^\circ, 43^\circ,$  and  $53^\circ$ , which are due to the (002), (10), and (004) diffractions of graphitic carbon. A comparison of the intensity of the “graphitic” peaks (Figure 2B) suggests a greater level of graphitic ordering for sample CR1300P. A greater level of graphitization in sample CR1300P is consistent with the higher CVD temperature (i.e., 1300 °C compared with

900 °C for sample CR900P) at which the sample was prepared. The nitrogen sorption isotherms of the powder carbon samples are shown in Figure 2C. The sorption isotherms suggest that sample CR1300P, which had a surface area of 639 m<sup>2</sup>/g and a pore volume of 0.84 cm<sup>3</sup>/g, is microporous. On the other hand, the isotherm of sample CR900P (surface area of 651 m<sup>2</sup>/g and pore volume of 0.93 cm<sup>3</sup>/g) suggests the presence of both micropores and textural mesopores. It is very clear therefore that, for the powder samples, the mesostructural ordering of the silica is to some extent replicated in the carbons.<sup>3,4,8,11</sup>

As mentioned above, CVD at 1300 °C generated large rod-like carbon particles (designated as CR1300R) that were distinct from the powder sample. Figure 3 shows SEM images of the large rod-like particles. Figure 3a,d indicates that ultralarge rods of length up to several millimeters and of diameter of 100–400 μm were present both before and after washing in HF. The large rods are mainly stand-alone, although some are loosely aggregated. Closer inspection indicates that the large rods are composed of aggregated spherical particles of diameter of 1–2 μm. The surface of the HF treated rods (Figure 3f) is much cleaner and free from nonspherical particles that are present prior to HF treatment (Figure 3c). The nonspherical particles have a rod-like appearance and are likely to be SBA-15 rods; this is supported by the fact that they are removed by the HF treatment. It is noteworthy that the spherical particles that make up the large rods are similar to the carbon spheres prepared via pyrolysis of hydrocarbons.<sup>9,10</sup> The presence of silica particles appears to cause the self-assembly of the carbon spheres into large rod-like particles.

TGA was used to assess the content of silica in large rod-like composites prior to HF treatment. The TGA curve, shown in Figure 4A, indicates that the large rods (before HF treatment) consist mainly of carbon with a silica content of ~4 wt % (equivalent to the residual mass at 1000 °C). Therefore, only a small amount of silica is present in the large rods. This suggests that the silica particles do not act as true templates<sup>2–8</sup> but rather as a substrate or as seeds for the self-assembly of carbon spheres into large rod-like macrostructures. The lack of a true hard-templating effect is consistent with the fact that the large rods have low textural properties: surface area of ~30 m<sup>2</sup>/g and pore volume of ~0.04 cm<sup>3</sup>/g. These textural properties are much lower than those of the powder sample (CR1300P) for which there is a templating effect. The differential thermogravimetric (DTG) profile in Figure 4 shows that the carbon burn off is centered at ~880 °C. The relatively high burn off temperature suggests that the carbon rods have turbostratic/graphitic characteristics. This suggestion is based on the assumption that graphitic carbons are thermally more stable compared to amorphous carbons.<sup>11,14</sup> The XRD patterns of the large carbon rod sample (CR1300R) and the powder sample (CR1300P) are compared in Figure 5A. XRD peaks at  $2\theta = 26^\circ, 43^\circ,$  and  $53^\circ$  due to the (002), (10), and (004) diffractions of

(14) (a) Kim, T. W.; Park, I. S.; Ryoo, R. *Angew. Chem., Int. Ed.* **2003**, *42*, 4375. (b) Xia, Y.; Mokaya, R. *Chem. Mater.* **2005**, *17*, 1553. (c) Yang, H.; Yan, Y.; Liu, Y.; Zhang, F.; Zhang, R.; Meng, Y.; Li, M.; Xie, S.; Tu, B.; Zhao, D. Y. *J. Phys. Chem. B* **2004**, *108*, 17320.



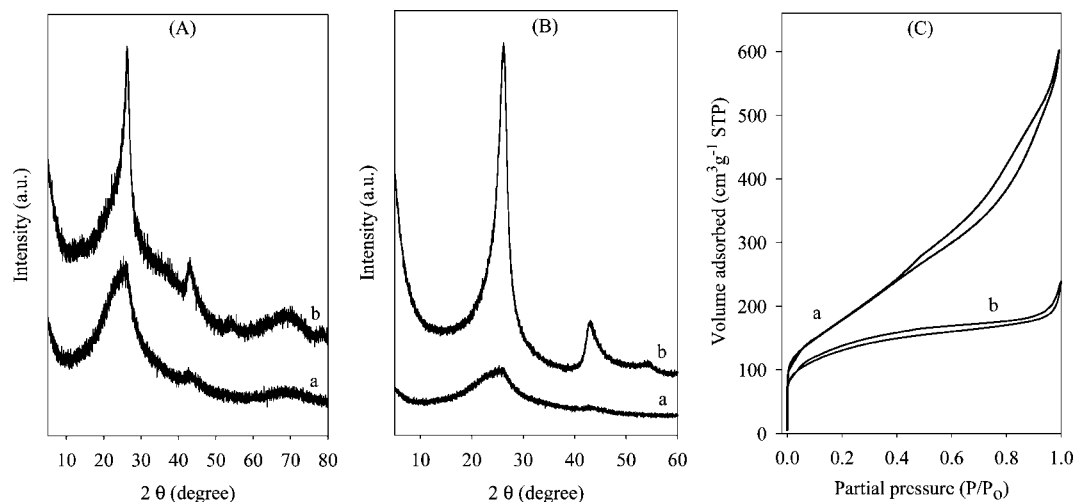


**Figure 2.** XRD patterns (A, B) and nitrogen sorption isotherms (C) of carbon materials; (a) CR900P and (b) CR1300P, before (A) and after (B, C) HF wash.

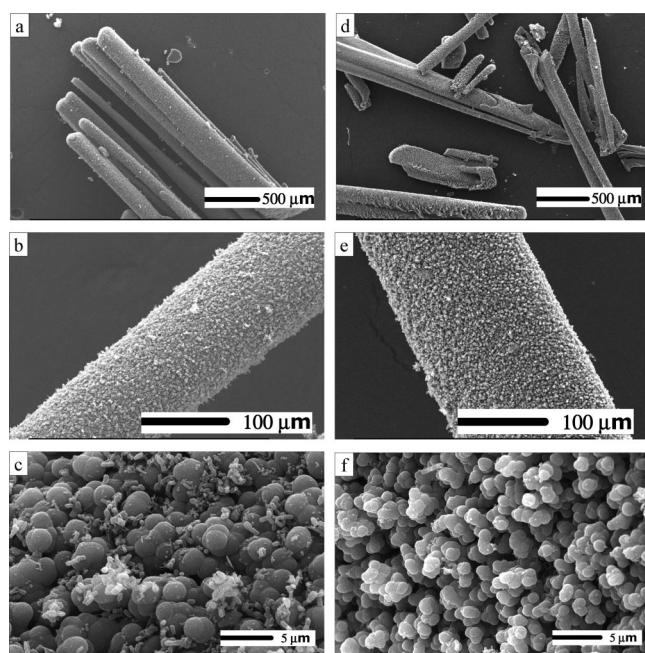


**Figure 3.** SEM images of large rod-like carbon material (sample CR1300R), before (a, b, c) and after (d, e, f) HF wash.

turbostratic/graphitic carbon appear for both samples. However, the peak intensity is much higher for the large rod sample (CR1300R) compared to that for the powder sample (CR1300P), implying a higher graphitic ordering in the rods.

Several experiments were performed under CVD conditions at 1300 °C to probe the formation mechanism of the large carbon rods. Because the large carbon rods were mainly observed on the exposed regions of the alumina boat, an experiment was carried out to assess the effect of the amount of silica used. Mesoporous silica SBA-15 rods were used under the same CVD conditions (i.e., CVD at 1300 °C for 10 h) except that the amount of silica was much lower (i.e., the minimum amount required to just cover the bottom of the alumina boat). Despite the use of much lower amounts of silica, large carbon rods were still generated. To further investigate the link between the silica and the formation of the large carbon rods, two more experiments were performed

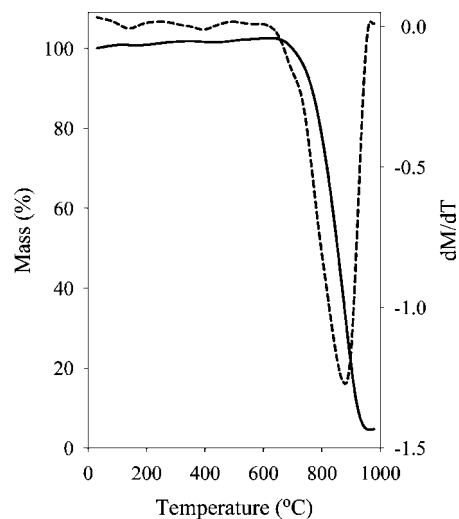


**Figure 4.** TGA curve (solid line) and corresponding DTG profile (dashed line) of large rod carbon (sample CR1300R) before HF treatment.

under similar CVD conditions except (i) with SBA-15 spheres (rather than SBA-15 rods) or (ii) with no silica at all (i.e., an empty alumina boat). Interestingly, large carbon rods (designated as CS1300R) were obtained with SBA-15 spheres. However, only powdered carbon (designated as C1300P) was obtained in the absence of any silica. Figure 6 shows the SEM images of the large carbon rods (CS1300R) obtained using SBA-15 spheres and of the carbon powder (C1300P) obtained in the absence of silica (empty alumina boat). The SEM images indicate that both the large rod CS1300R and the powder C1300P samples are made up of spheres. On the basis of these results, it is suggested that silica particles (either rods or spheres) are essential for the formation of the large carbon rods.

Figure 5B shows XRD patterns of carbon materials prepared under various conditions. It is noteworthy that there was no significant difference in the XRD patterns before and after HF treatment (see Figure 1 in the Supporting Information), which implies that only small amounts of silica are occluded in the rods (for sample C1300P, no HF treatment is required because no silica template was employed!). This

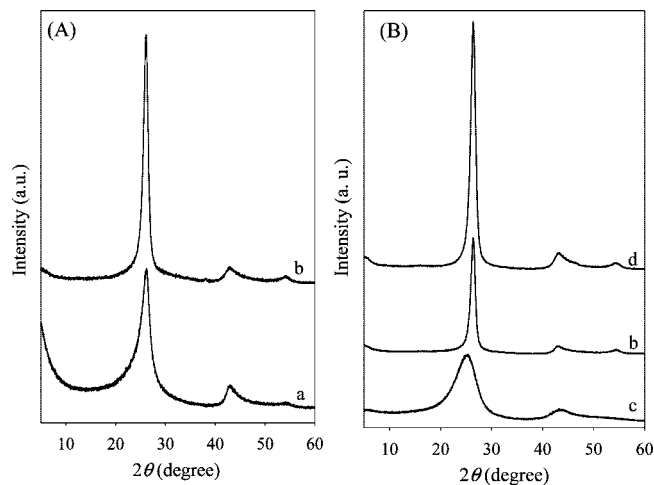


**Figure 5.** XRD patterns of carbon materials obtained via CVD at 1300 °C for 10 h; (a) powder sample CR1300P, (b) large rod sample CR1300R, (c) powder sample C1300P prepared without any silica, and (d) large rod sample CS1300R prepared using SBA-15 spheres.

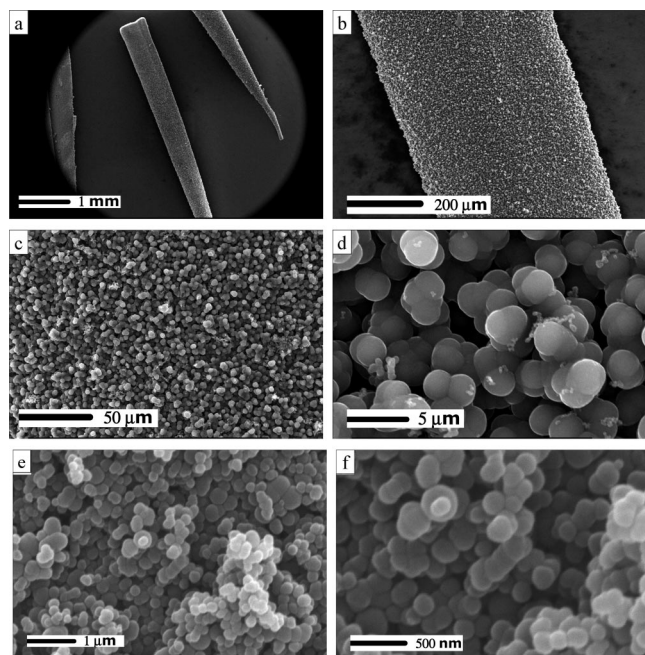


**Figure 6.** SEM images of carbon materials obtained at 1300 °C for 10 h; (a–d) using mesoporous silica SBA-15 spheres (sample CS1300R) and (e, f) in the absence of any silica (sample C1300P).

is in agreement with the TGA data in Figure 4, which shows that the carbon rods contain less than 4 wt % silica. The effect of CVD duration on the formation of large carbon rods was investigated by performing CVD for 5 h rather than 10 h. Large carbon rods were still obtained but in lower quantities. Figure 7 shows the SEM images of the 5 h carbon rods, confirming that they were also made up of spheres. The length of the 5 h carbon rods was similar to that of 10 h carbon rods, and the XRD patterns (see Figure 2 in the Supporting Information) imply comparable levels of graphitization for 5 h and 10 h carbon rods.

Our investigations show that silica particles are essential for the formation of the large carbon rods. We tentatively propose that the silica particles act as a substrate or as seeds for the self-assembly of carbon spheres that are generated

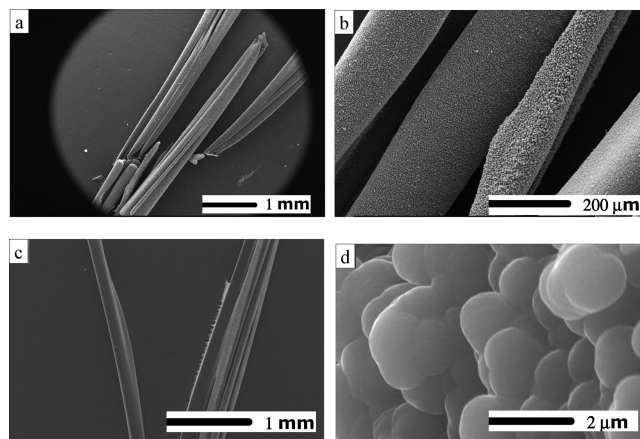


**Figure 7.** SEM images of large rod carbon obtained via CVD at 1300 °C for 5 h using mesoporous silica SBA-15 rods, before (a, b) and after (c, d) HF wash.

under the prevailing CVD conditions.<sup>9,10</sup> The carbon rods were mainly observed on the exposed parts of the sample holder. It is likely that this phenomenon arises when silica particles (rods or spheres), which are displaced by the gas flow of the CVD process, act as deposition points for carbon spheres.<sup>9,10</sup> Further deposition of carbon spheres, as determined by the directional flow of the carbon precursor, enables the accretion of more spheres in a set manner. This directed accretion of carbon spheres eventually generates elongated carbon rods. The proposed tentative mechanism is supported by the observation that the large rods, when directly anchored onto the sample holder, appeared to grow toward the source of the carbon precursor (i.e., against the flow of the acetonitrile). Such a growth pattern would facilitate optimal contact between the growing rod and the carbon precursor (acetonitrile) and enable the formation of large macrostructures made up of the deposited carbon spheres. In such a scenario, only small amounts of silica particles are needed to act as seeds or “glue” for the carbon rods. It is noteworthy that the packing of the carbon spheres (contact between the spheres) is sufficiently compact to allow the formation of large self-supporting carbon rods after removal of the silica (Figures 3, 6, and 7). The large rods may therefore be considered as being continuously homogeneous carbon materials.

The carbon rods exhibited significant mechanical stability that allowed easy handling. The rods did not break when touched or compacted under hand pressure. Even moderate pressure with a spatula did not crush the rods. To assess the connectivity within the carbon rods, we measured their electrical conductivity. The electrical conductivity of individual carbon rods was measured at room temperature as follows: the carbon rod under investigation was pasted with silver between two isolated gold coated glass substrates (see Figure 3 in the Supporting Information). The potential and current were supplied and monitored by a CH Instruments electrochemical workstation. Several measurements involving different rods were performed for each assessed sample. The conductivity of the carbon rods was found to be typically 600–800 S m<sup>-1</sup> and more generally in the range 180–1360 S m<sup>-1</sup>. We observed some variation between samples,

although rods from the same sample generally gave similar conductivity values.

The high electrical conductivity observed for the rods is due to their graphitic nature and, more importantly, is an excellent indication of the compactness within the rods. The conductivity of the carbon rods is higher than that ( $30\text{--}155\text{ S m}^{-1}$ ) previously reported for silica templated graphitic mesoporous carbons.<sup>7c,15</sup> In addition to the high electrical conductivity, the present rods have the added advantage of not requiring any postsynthesis compaction prior to analysis or use as electrical conductors. Overall, the fact that significant electrical conductivity is observed for the carbon rods indicates that they are compact with good contact between the constituent spheres. Indeed, electrical conductivity of up to  $1360\text{ S m}^{-1}$  is remarkable considering the self-assembled nature of the rods and the fact that they are prepared at only  $1300\text{ }^\circ\text{C}$ . The conductivity of the rods is higher than that ( $420\text{ S m}^{-1}$ ) of mesoporous carbons graphitized at a much higher temperature of  $2300\text{ }^\circ\text{C}$ .<sup>15c</sup> Improvements in conductivity are possible by raising the CVD temperature at which the carbon rods are prepared. The length and diameter of the rods may also be modified by changing the synthesis conditions (e.g., gas flow rate, CVD duration).

#### 4. Conclusions

In summary, we have fabricated new graphitic carbon macrostructures in the form of mechanically robust

ultralarge rods, which exhibit high thermal stability and electrical conductivity. The rods are obtained during pyrolysis of acetonitrile under CVD conditions at  $1300\text{ }^\circ\text{C}$  in the presence of mesoporous silica particles. The rods grow to attain a length of up to  $5\text{ mm}$  and have a diameter typically in the range  $100\text{--}400\text{ }\mu\text{m}$ . The proposed mechanism of formation of the large rods involves self-assembly of carbon spheres (of diameter  $1\text{--}2\text{ }\mu\text{m}$ ) that are generated directly from the acetonitrile. The presence of silica particles is essential for the formation of large rods. The silica particles function as a substrate (seed or “glue”) for the growth of the carbon rods. The spheres comprising each rod are closely packed thus generating self-supporting macrostructures that are compact and mechanically robust after removal of the silica particles. The rods have high thermal stability and electrical conductivity. The CVD process reported here allows for the direct fabrication of self-supporting and mechanically robust millimeter-sized carbon rods that may be directly used without any postsynthesis formulation.

**Acknowledgment.** The authors are grateful to the EPSRC for financial support.

**Supporting Information Available:** Three additional figures: XRD patterns of carbon materials and a photograph showing the setup for the electrical conductivity measurements (PDF). This material is available free of charge via the Internet at <http://pubs.acs.org>.

CM702049C

- 
- (15) (a) Yang, H.; Shi, Q.; Liu, X.; Xie, S.; Jiang, D.; Zhang, F.; Yu, C.; Tu, B.; Zhao, D. Y. *Chem. Commun.* **2002**, 2842. (b) Kim, C. H.; Lee, D. K.; Pinnavaia, T. J. *Langmuir* **2004**, *20*, 5157. (c) Fertes, A. B.; Alvarez, S. *Carbon* **2004**, *42*, 3049. (d) Su, F.; Zhao, X. S.; Wang, Y.; Lee, J. Y. *Microporous Mesoporous Mater.* **2007**, *98*, 323.